IGI Poseidon

ERM Asprofos engineering

PROJECT:

# EastMed Pipeline Project


| | |
|---|---|
| Document Title: | EastMed Greek Section – Environmental and Social Impact Assessment |
| Document Subtitle: | Annex9A.2- Air dispersion model for Achaia Compressor Station |
| Project Document No: | PERM-GREE-ESIA-A09_0004_0_Annex9A2 |

| Document details | |
|---|---|
| Document title | EastMed Greek Section – Environmental and Social Impact Assessment |
| Document subtitle | Annex9A.2 - Air dispersion model for Achaia Compressor Station |
| Company | IGI Poseidon |
| Author | DEMOKRITOS |
| Project | EastMed Pipeline Project |
| Project Document No. | PERM-GREE-ESIA-A09_0004_0_Annex9A2 |
| Date | 03/06/2022 |
| Version | 00 |

**Document history**

| Revision | Author | Reviewed by | Approved by | Date | Status |
|---|---|---|---|---|---|
| 00 | DEMOKRITOS | ASPROFOS | IGI POSEIDON | 03/06/2022 | For submission to Authorities |

## Table of Contents



## List of Tables

## List of Figures

## External cooperation

This document was drafted with the cooperation of:

- National Center for Scientific Research ''Demokritos''

# ANNEX 9A.2 AIR DISPERSION MODEL FOR ACHAIA COMPRESSOR STATION

# 9A.2.1 INTRODUCTION

## 9A.2.1.1 SUMMARY

The Environmental Research Laboratory (EREL) of the National Centre for Scientific Research "Demokritos" performed the modelling study of the atmospheric dispersion of NOx, and CO concentrations from the future installation of the Compression of Natural Gas Station, CS3, part of the EastMed pipeline, in the Achaia area, in the north-western part of the Peloponnese peninsula.

The study was carried out for ASPROFOS Engineering S.A. by the following EREL personnel:

- Vlachogianni Diamando, M.Sc., Ph.D
- Sfetsos Athanasios., Ph.D
- Gounaris Nikolaos., M.Sc.
- Emmanouil George, PhD.
- Karozis Stelios, M.Sc., Ph.D

## 9A.2.1.2 AIM OF THE REPORT

The scope of this study is to investigate the impact of the dispersion of Nitrogen Oxides ($NO_x$) and Carbon Monoxide (CO) on the atmospheric quality from the future installation of the gas Compression Stations (CS3), in the area of Achaia, aimed at providing additional compression required, in the Natural Gas transmission system of the EastMed pipeline. During the operation of the onshore installation of the pipeline, pollutant gases are emitted to the atmosphere as a result of the combustion of natural gas in the compression station through Gas Turbines (GT) according to the standard of the European Association for the Streamlining of Energy Exchange – gas (EASEE-gas). Consequently, emissions of particulate matter (PM) and sulfur dioxide ($SO_2$) are negligible. According to the European Best available techniques Reference document (BREFs) developed under the IPPC Directive for large combustion installations, CO and $NO_x$ are the only gas pollutants emitted that should be taken into account in air dispersion modelling studies.

In the current modelling study, the 3-dimensional computer modelling tools were used with appropriate methodology[2] developed by the Environmental Research Laboratory (EREL) of the NCSR "Demokritos". The position and geometry data about the stacks, emission rates of $NO_x$ and CO were provided to EREL by Asprofos S.A. based on construction information.

The meteorological data for the area of interest were retrieved by EREL. The data related to the topography of the area were extracted from the Geographic Information System (ARC GIS) available at EREL. The basic computational and analysis steps followed are listed below:

- Processing of the available data, preparation of the input files for the dispersion model regarding the topography (ARC.GIS) and the meteorology of the area.
- Meteorological computational calculations to obtain the characteristic weather types of the area of interest and the respective 3-Dimensional meteorological fields (WRF model).
- Modelling calculations of the atmospheric dispersion of the emissions of $NO_x$ and CO from the gas compression station (HYSPLIT model).
- Analysis and evaluation of the model results on the near ground distribution of the $NO_x$ and CO concentrations.
- Modelled near ground concentrations of the pollutants were compared against European air quality standards (2008/50/EC), adopted by Greek legislation, considering ambient background levels and potential receivers (populated places).

## 9A.2.2 PREPARATION OF THE INPUT DATA

This part involves the preparation of the input data files for the atmospheric dispersion model. For the specific study, the necessary data include the topography and meteorological fields of the area of interest.

2 D. Vlachogiannis, A. Sfetsos, N. Gounaris and A. Papadopoulos," Investigation of atmospheric dispersion of gas compounds from an industrial installation over a realistic topography", 17th International Conference on Harmonisation within Atmospheric Dispersion Modelling for Regulatory Purposes, 9-12 May 2016, Budapest.

### 9A.2.2.1 TOPOGRAPHY AND MODELLING DOMAIN

The geographical coordinates of the emission sources of the gas compression station CS3 in the area of Achaia (regional unit of north-western Peloponnese) on Greek Geodetic Reference System GGRS87 (X,Y) and latitude /longitude are shown on Table A2- 1.

Table A2- 1 Geographic coordinates of the centroid of the industrial field and each stack of GS3.

| UNIT | X (m) | Ψ (m) | Longitude (°) | Latitude (°) |
|---|---|---|---|---|
| Centroid of industrial field | 283508.314652 | 4200265.8445 | 21.539000 | 37.926825 |
| CS3 _1 | 283525.240 | 4200323.537 | 21.538710 | 37.927353 |
| CS3 _2 | 283512.749 | 4200282.914 | 21.538580 | 37.926984 |
| CS3 _3 | 283500.307: | 4200242.273 | 21.538451 | 37.926615 |
| CS3_4 | 283487.840 | 4200201.643 | 21.538321 | 37.926246 |

Prepared by Demokritos on behalf of ASPROFOS, 2022.

The computational domain extent was set to 30 × 30 $km^2$ to include as many as possible neighbouring urban areas of the area (see Figure A2-1). The topography of the area around the CS3 location is smooth with low elevation and plain areas westwards and higher altitudes in the eastern direction.

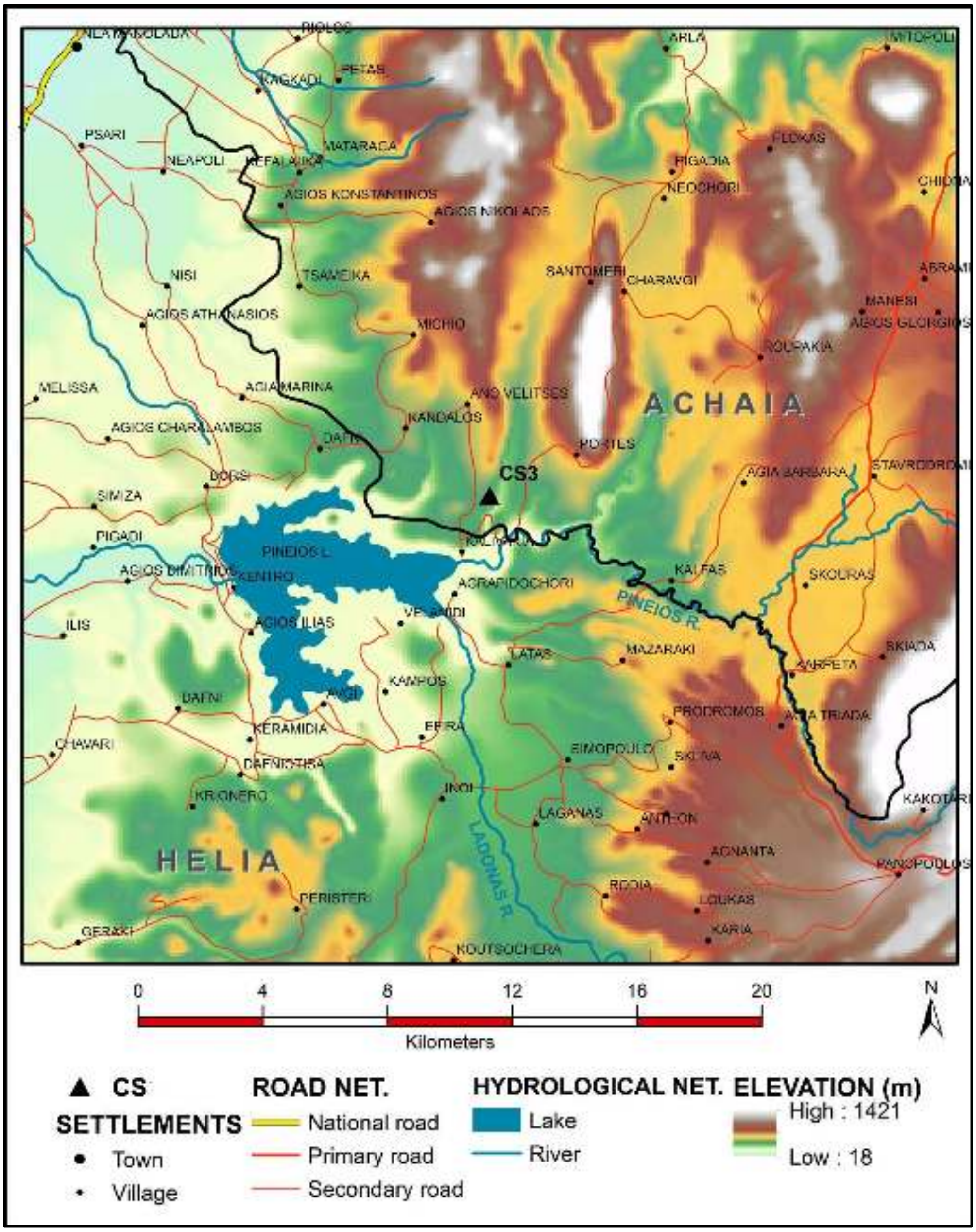


Prepared by Demokritos on behalf of ASPROFOS, 2022.

Figure A2-1 Topography map of the computational domain of size 30 x30 km2. The gas compression station CS3 (Achaia) is located in the centre of the domain.

### 9A.2.2.2 METEOROLOGY AND CHARACTERISTIC WEATHER TYPES

The atmospheric dispersion models use as input data meteorological variables such as wind speed and wind direction, temperature, category of atmospheric stability, mixing layer height etc. The more complex models (like the one used in this study named HYSPLIT) use 3-dimensional meteorological fields as input. The discretised meteorological fields are calculated by prognostic and/or diagnostic models.

For the current study, meteorological data (vertical distribution of wind speed and direction, temperature, mixing layer height, humidity, precipitation, cloud cover etc) were extracted from the European Centre for Medium-Range Weather Forecasts (ECMWF) ERA-5 climate re-analysis dataset, (https://confluence.ecmwf.int/display/CKB/ERA5%3A+data+documentation), available at 3-hourly intervals.

#### *9A.2.2.2.1 Characteristic Weather Types over the study area*

To calculate the average levels and the maximum values of the pollutant concentrations from a future installation in the atmosphere on an annual, daily and hourly basis, the procedure of identifying the typical meteorological conditions or else characteristic weather types (CWT) of the area of interest was followed. The prevailing meteorological conditions or in other words characteristic weather types were obtained using the methodology of Sfetsos et al. (2005)[3]. The specific methodology was applied on ERA5 reanalysis data of large scale, as referenced above, covering a period of eleven years (2010-2020). The analysis revealed the prevailing weather conditions in the defined computational domain and the corresponding frequency of occurrence (in percentage) per year. Each weather condition was assigned a characteristic or else typical day (24-hour).

The results showed that the area of study is characterised by eleven (11) in total weather types (see Table A2- 2). Table A2- 3, summarises the meteorological conditions from the global reanalysis model, which characterise each typical weather day of the region.

Table A2- 2 Characteristic weather types (CWT) and percentage of their frequency of occurrence within a typical year in the area of Achaia.

| CS3 | |
|---|---|
| Typical weather type | Frequency Percentage of occurrence in a year (%) |
| 1 | 13.06 |
| 2 | 5.56 |
| 3 | 6.31 |

[3] A. Sfetsos, D. Vlachogiannis, N. Gounaris, and A. K. Stubos, (2005). On the identification of representative samples from large data sets with application to synoptic climatology, Theor. Appl. Climatol. 82, 177–182.

| CS3 | |
|---|---|
| Typical weather type | Frequency Percentage of occurrence in a year (%) |
| 4 | 9.80 |
| 5 | 15.40 |
| 6 | 8.60 |
| 7 | 3.50 |
| 8 | 7.54 |
| 9 | 5.57 |
| 10 | 8.68 |
| 11 | 15.98 |

Prepared by Demokritos on behalf of ASPROFOS, 2022.

Table A2- 3 Prevailing meteorological conditions during the 11 characteristic weather types (CWT) in the domain of Achaia: horizontal component of wind speed, u (m/s), vertical component of wind speed v (m/s), (at 850 mb and 10 meters above mean sea level, a.m.s.l.

| CWT | u10 (0 h) | u10 (12 h) | v10 (0 h) | v10 (12h) | T (0 h) | BLH (12 h) | |
|---|---|---|---|---|---|---|---|
| 1 | -0.712 | 2.551 | -0.627 | -0.297 | 286.35 | 918.05 | - |
| 2 | -1.490 | 0.335 | 0.180 | 1.922 | 287.15 | 759.76 | - |
| 3 | -0.742 | 1.283 | -0.502 | -0.705 | 291.96 | 1544.43 | - |
| | u10 (0 h) | u10 (12 h) | v10 (0 h) | v10 (12h) | T (0 h) | T (12 h) | BLH (12 h) |
| 4 | -0.951 | 2.256 | -0.058 | -0.238 | 284.53 | 298.49 | 1311.20 |
| 5 | -0.768 | 2.416 | 0.020 | 0.631 | 281.72 | 291.00 | 1053.22 |
| | u10 (0 h) | u10 (12 h) | v10 (0 h) | v10 (12h) | T (0 h) | BLH (12 h) | - |
| 6 | -0.106 | 2.948 | -0.354 | -1.218 | -0.819 | -0.618 | - |
| 7 | -1.653 | -0.631 | -0.430 | -1.270 | -0.656 | -0.956 | - |
| 8 | -0.233 | 3.104 | -0.483 | -1.013 | -0.955 | -0.172 | - |
| 9 | -1.066 | 1.385 | -0.512 | -0.415 | -1.316 | -0.672 | - |
| | u10 (0 h) | u10 (12 h) | v10 (0 h) | v10 (12h) | T (0 h) | T (12 h) | BLH (12 h) |
| 10 | -1.450 | 0.432 | 1.077 | 1.955 | 282.63 | 286.14 | 861.30 |
| 11 | -1.133 | 1.976 | 0.076 | -0.899 | 279.05 | 285.18 | 858.95 |
| CWT | RH (0 h) | RH (12 h) | u850 (0 h) | - | - | - | - |
| 1 | 84.70 | 56.52 | 0.723 | - | - | - | - |
| 2 | 83.20 | 73.38 | 4.994 | - | - | - | - |

| | | | | | | | |
|---|---|---|---|---|---|---|---|
| 3 | 72.70 | 37.70 | 1.591 | - | - | - | - |
| | RH (0 h) | RH (12 h) | u850 (0 h) | v850 (0 h) | - | - | - |
| 4 | 81.31 | 41.80 | -1.119 | -1.595 | - | - | - |
| 5 | 93.94 | 60.94 | 5.354 | -2.536 | - | - | - |
| | RH (0 h) | u850 (0 h) | v850 (0 h) | - | - | - | - |
| 6 | 84.71 | 0.955 | -3.722 | - | - | - | - |
| 7 | 51.31 | -7.226 | -6.193 | - | - | - | - |
| 8 | 92.31 | 2.454 | -5.499 | - | - | - | - |
| 9 | 72.75 | -2.402 | -2.566 | - | - | - | - |
| | RH (0 h) | RH (12 h) | u850 (0 h) | v850 (0 h) | - | - | - |
| 10 | 88.51 | 67.52 | 0.847 | 8.792 | - | - | - |
| 11 | 83.16 | 62.03 | 1.818 | -0.990 | - | - | - |

Prepared by Demokritos on behalf of ASPROFOS, 2022.

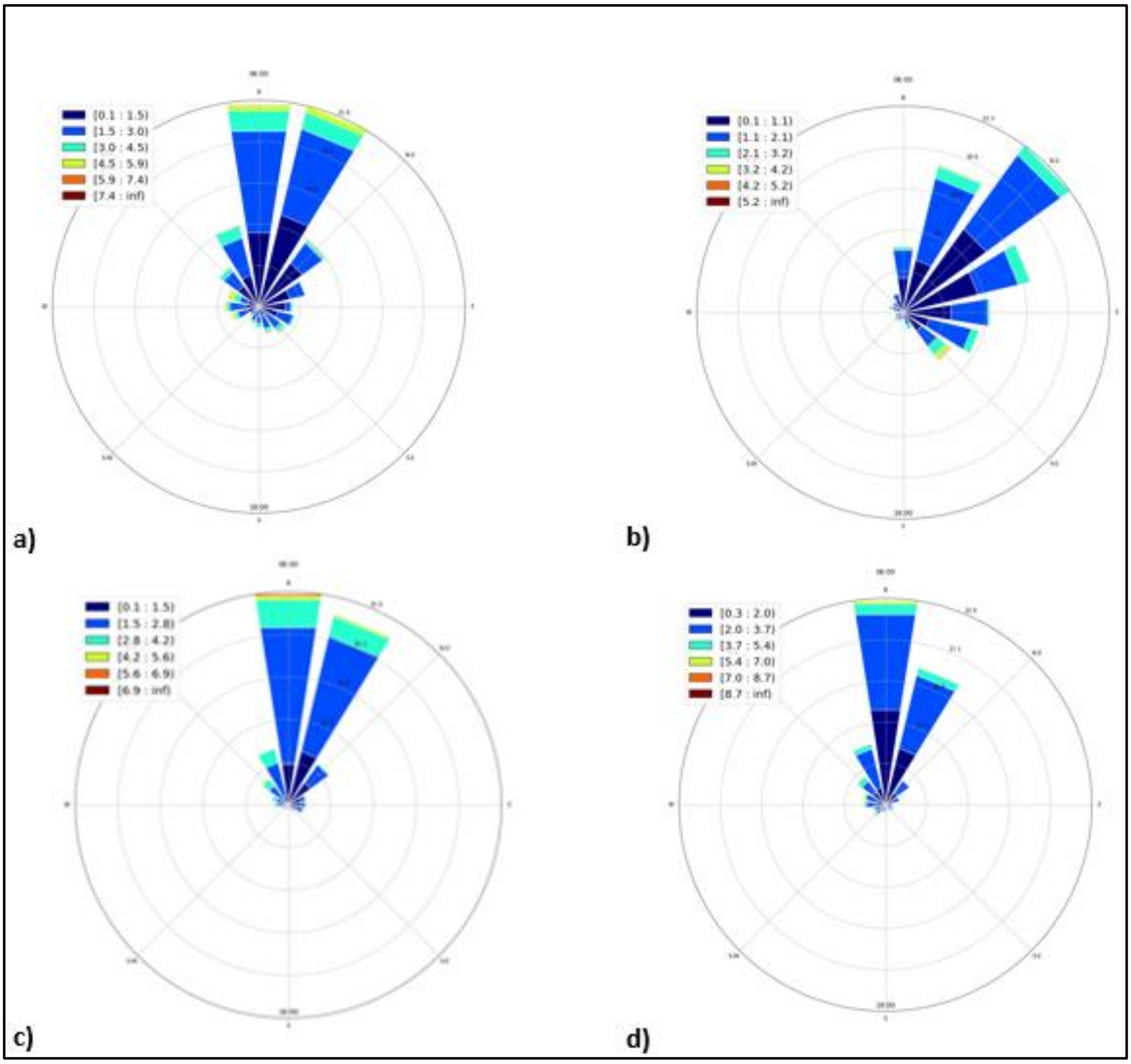


Prepared by Demokritos on behalf of ASPROFOS, 2022.

**Figure A2-2 Wind rose diagrams in the area of Achaia, centred at the location of CS3, at 10 m a.s.l. and 12:00, for a) spring, b) summer, c) autumn and d) winter.**

Figure A2-2 presents the calculated wind rose diagrams at the location of the CS3, at 10 meters height for a typical year, calculated using ERA5 data. The concentric circles correspond to the relative frequency of each wind direction and the colour gradation is related to the percentage (%) of the wind speed per direction.

### *9A.2.2.2.2 Weather conditions description*

The description of the weather conditions prevailing during each characteristic weather type of Table A2- 2 (CWT) is provided below.

- CWT1
  Relative high pressures are covering the area of study, resulting to good weather during this autumn day, low to moderate northerly wind speeds and temperature up to 23-25 degrees Celsius during noon.
- CWT2
  Low pressure system affects the Greek area with rainy weather accompanied with temporary thunderstorms in the area of interest during this typical autumn day. The winds are light to moderate from variable directions, veering in the afternoon to moderate westerlies, while temperature rises to 21-23 degrees Celsius.
- CWT3
  A shallow low-pressure system is passing south of Greece causing rainy weather locally at the area of interest during this autumn day. North-westerly moderate winds are prevailing over the area and temperature is up to 27-29 degrees Celsius during early afternoon.
- CWT4
  In this spring day, high pressures are covering the area with fair weather, light variable winds and maximum temperature reaching 26-28 degrees Celsius.
- CWT5
  Smooth barometric field is affecting the weather of the country with local clouds over the study area during this spring typical day. The winds are variable and temporarily westerlies of light to moderate intensity and the temperature up to 14-16 degrees Celsius during noon.
- CWT6
  High pressures associated with fine weather are affecting the area during this typical summer day, resulting to increased temperature 31-33 degrees Celsius during early afternoon and light winds, which temporarily, the hot period of the day, veer to westerlies up to moderate.
- CWT7
  High pressures field is covering the country, with fine weather in the Achaia region during this typical summer day. The winds blow from northeast directions light to moderate, and the temperature is climbing to 33-35 degrees Celsius at noon.
- CWT8
  High pressures prevail during this typical summer day resulting to fair weather at the area of study. The winds are of low intensity from variable directions, when during the hot part of the

day they are north-westerlies up to moderate and the temperature reaches 31-33 degrees Celsius.

- CWT9
  High pressures field and fine weather over the area of interest during this typical summer day. The winds blow from north directions light to moderate, while the temperature is high reaching 34-36 degrees Celsius at mid-day.
- CWT10
  A low barometric atmospheric system is moving eastwards, causing rains and thunderstorms the area of interest on this winter day. The winds are blowing from south-eastern directions light to moderate and temperature rises to 14-16 degrees Celsius during noon.
- CWT11
  Smooth barometric system is moving south of Greece, affecting with light rain the Achaia region during this typical winter day. The winds are light variable and gradually north-westerlies moderate, while the temperature reaches 12-14 degrees Celsius.

#### *9A.2.2.2.3 Atmospheric model WRF*

The prognostic meteorological model Weather Research Forecasting (WRF-ARW) version 3.6.1 (Skamarock et al., 2008)[4] was set-up and used for the calculation of the 3-dimensional meteorological fields. The WRF model calculated the 3-dimensional meteorological fields of the region of interest with horizontal and temporal resolution of 1 × 1 $km^2$ and 1-hour, respectively. The ERA-5 data for the determined characteristic weather days were used as initial and boundary conditions to the meteorological model (WRF). The model simulations were performed for the 11 characteristic weather days (CWT).

As an example of the WRF results, Figure A2-3 - Figure A2-4 display examples of the WRF calculated 3-dimensional temperature and wind fields for CWT1 (autumn), CWT4 (spring), CWT6(summer) and CWT10 (winter) at 12:00 hr and 24:00 hr. The calculated meteorological fields were consequently used as input to the dispersion model.

4 Skamarock, W. C., J. B. Klemp, J. Dudhia, D. O. Gill, D. M. Barker, M. G. Duda, X.-Y. Huang, W. Wang, and J. G. Powers, 2008: A description of the Advanced Research WRF version 3. NCAR Technical Note 475, http://www.mmm.ucar.edu/wrf/users/docs/arw_v3.pdf.

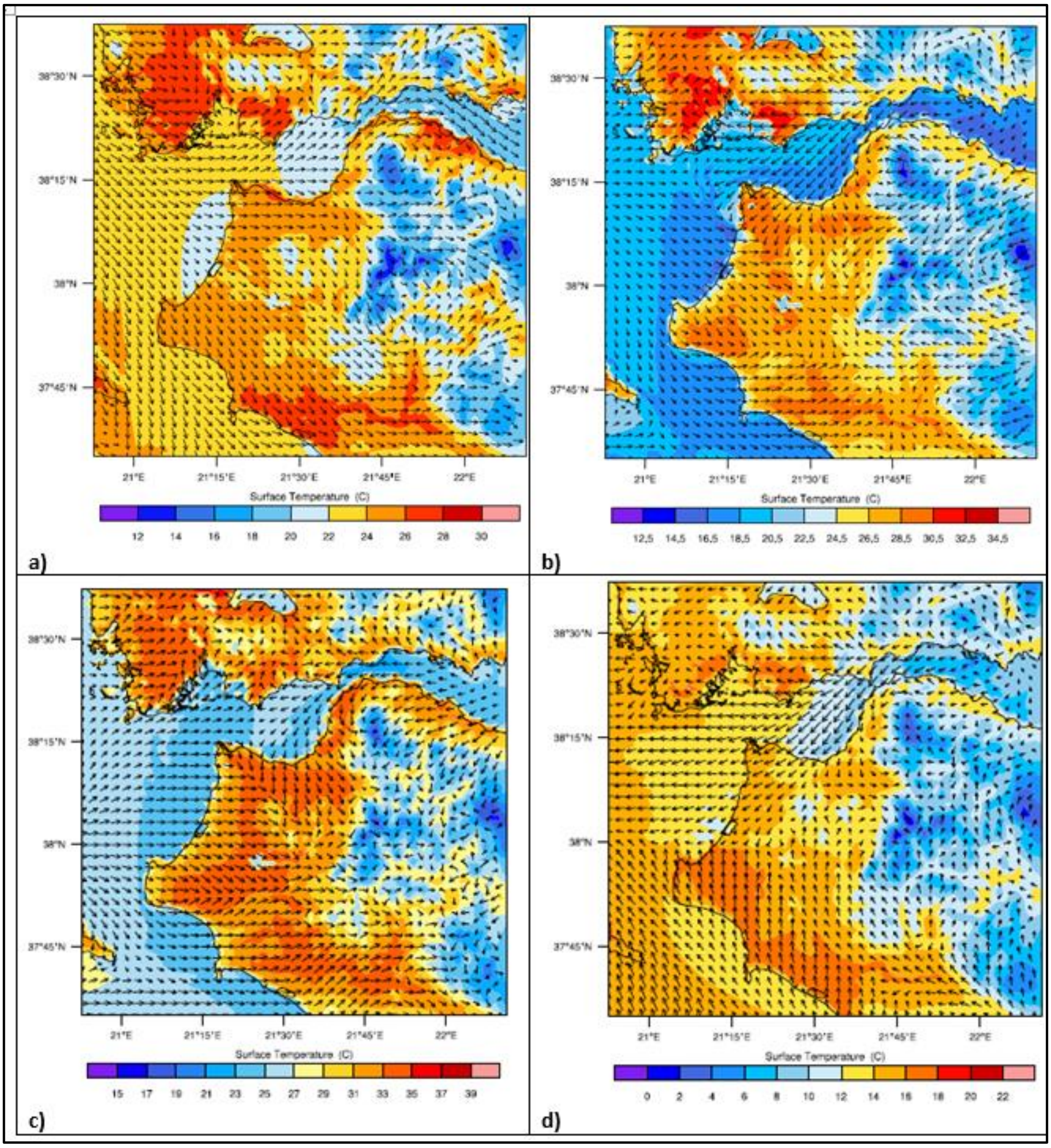


Prepared by Demokritos on behalf of ASPROFOS, 2022.

Figure A2-3 WRF calculated near surface temperature and wind fields in the area of Achaia (CS3), at 12:00hr for: a) CWT1(autumn), b) CWT4 (spring), c) CWT6 (summer) and d) CWT10 (winter).

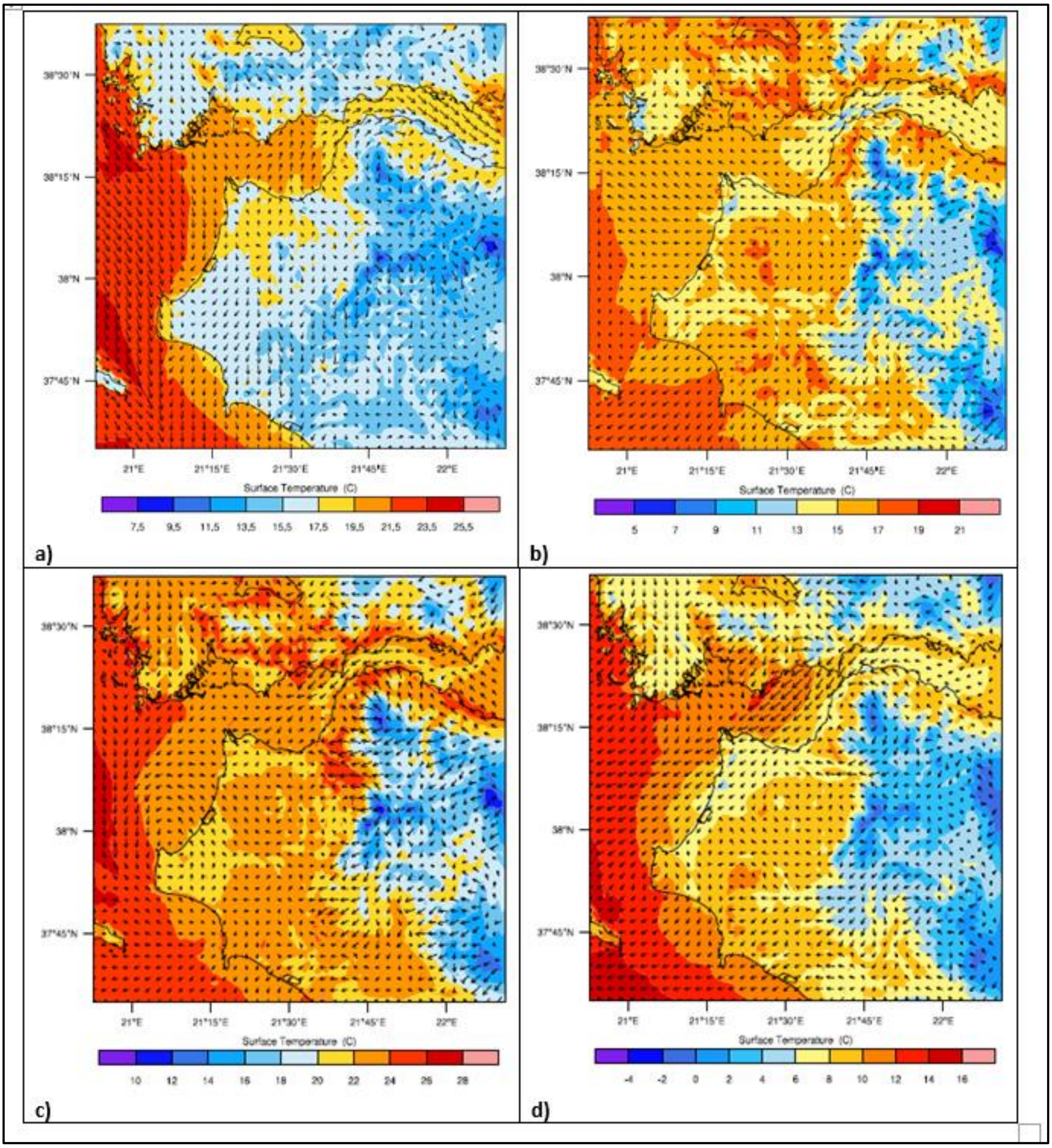


Prepared by Demokritos on behalf of ASPROFOS, 2022.

Figure A2-4 WRF calculated near surface temperature and wind fields in the area of Achaia (CS3, at 24:00hr for: a) CWT1(autumn), b) CWT4 (spring), c) CWT6 (summer) and d) CWT10 (winter).

### 9A.2.2.3 SIMULATION OF THE DISPERSION OF THE POLLUTANTS

This chapter presents the preparation of the input data for the atmospheric dispersion model HYSPLIT (Hybrid Single Particle Lagrangian Integrated Trajectory Model) used in the present study.

#### *9A.2.2.3.1 The Dispersion Model*

The HYSPLIT model is the newest version of a complete system for computing simple air parcel trajectories to complex dispersion and deposition simulations. As a result of a joint effort between NOAA and Australia's Bureau of Meteorology, the model has been used for several applications (https://ready.arl.noaa.gov/HYSPLIT.php ). The Air Resources Laboratory’s HYbrid Single-Particle Lagrangian Integrated Trajectory (HYSPLIT) model is a complete system for computing both simple air parcel trajectories and complex dispersion and deposition simulations. The model calculation method is a hybrid between the Lagrangian approach, which uses a moving frame of reference as the air parcels move from their initial location, and the Eulerian approach, which uses a fixed three-dimensional grid as a frame of reference. In the model, advection and diffusion calculations are made in a Lagrangian framework following the transport of the air parcel, while pollutant concentrations are calculated on a fixed grid. The model is designed to support a wide range of simulations related to the atmospheric transport and dispersion of pollutants and hazardous materials, as well as the deposition of these materials onto the Earth’s surface.

##### *9A.2.2.3.1.1 Data of the pollutant emissions from GS3*

The compression station is designed to comprise three stacks (plus 1 spare) – Gas Turbines of 17.5 MW each (in ISO conditions), identical in characteristics and emission data. The spare turbine of CS3 was not included in the dispersion study. The computational study simulated the maximum operation of GS3 for in total 8,585 hours.

Table A2- 4 presents the data on the geometric characteristics of the stacks and the gas flow properties of the emission source. Table A2- 5 provides the emission values of the pollutants.

Table A2- 4 Technical data on emission sources from CS3.

| Number of stacks | Stack Geometric characteristics | | Exit gas Temperature (°C) | Turbine Exhaust gas flow rate (kg/h) | Turbine Exhaust gas density (kg/m³) |
|---|---|---|---|---|---|
| | Height (m) | Size (m) | | | |
| 3 | 20 | 2.6 × 3.8 | 492.0 | 180,000 | 0.65 |

Prepared by Demokritos on behalf of ASPROFOS, 2022.

Table A2- 5 Data of NOx and CO from each gas turbine of CS3.

| Pollutant | Pollutant concentration limit in exhaust mg/Nm³ | Emission rates of the pollutants kg/h |
|---|---|---|
| $NO_x$ (as $NO_2$) | 31 | 3.7 |
| CO | 20 | 2.2 |

Prepared by Demokritos on behalf of ASPROFOS, 2022.

## 9A.2.3 ATMOSPHERIC DISPERSION CALCULATIONS

This section focuses on the analysis of the HYSPLIT model results of the concentration values of $NO_x$, and CO from GS3.

The concentrations of $NO_x$ were calculated on an hourly and annual basis to compare the modelled calculated results with the respective air quality limits as set by the legislation in force (MD 14122/549/E.103/2011 “Measures to improve air quality in compliance with the provisions of Directive 2008/50/EC "on the air quality and cleaner air for Europe" the European Parliament and Council of the European Union of 21 May 2008”). According to the current directive, the air quality limit for $NO_2$ for averaging period of 1 hour is set at 200 μg/m$^3$, not to be exceeded more than 18 times a calendar. On an annual average basis, the respective limit is 40 μg/m$^3$. The CO values were calculated as maximum daily 8 hour running mean concentrations for comparison with the respective air quality limit of 10 mg/m$^3$ (Directive 2008/50/EC).

The modelling approach was performed without the inclusion of the photochemical reactions which could reduce the concentrations of $NO_x$ and CO in the atmosphere for the reason of obtaining the maximum possible values in the domain. Moreover, detailed data on the compounds from high resolution inventories would be needed for a photochemical model, which were not available. Special attention was given to the populated areas around the location of the gas compression stations.

A field survey campaign was carried out during the period of 3/06/2021 - 14/07/2021 to investigate the ambient air quality conditions in the area of interest. Details about the field sampling can be found in the corresponding section of the report. Figure  A2-5 shows the location of the sampling sites and Table A2- 6, summarises the results from the field campaign. The measured data represent mean hourly concentrations of the period of approximately 6 weeks during the summer season.

The measurements showed that the hourly average background concentrations of both pollutants of interest were of very low values compared to those found in more heavily populated areas of the country. In particular, the CO ambient concentrations were mostly lower than the detection limit (0.6 mg/m$^3$) of the measuring device and analytical method except for two locations where the values were significant low (equal to 610 and 675 μg/m$^3$). Hence, the concentrations of the CO background could not be taken into account in the modelling study and were considered to be equal to zero. Furthermore, the hourly average NOx concentrations were lower than the detection limit (0.7 mg/m$^3$) except for some locations where the average value was significant low and equal to 0.88 μg/m$^3$. The very low ambient concentrations were considered negligible to be included as background to the modelling study.

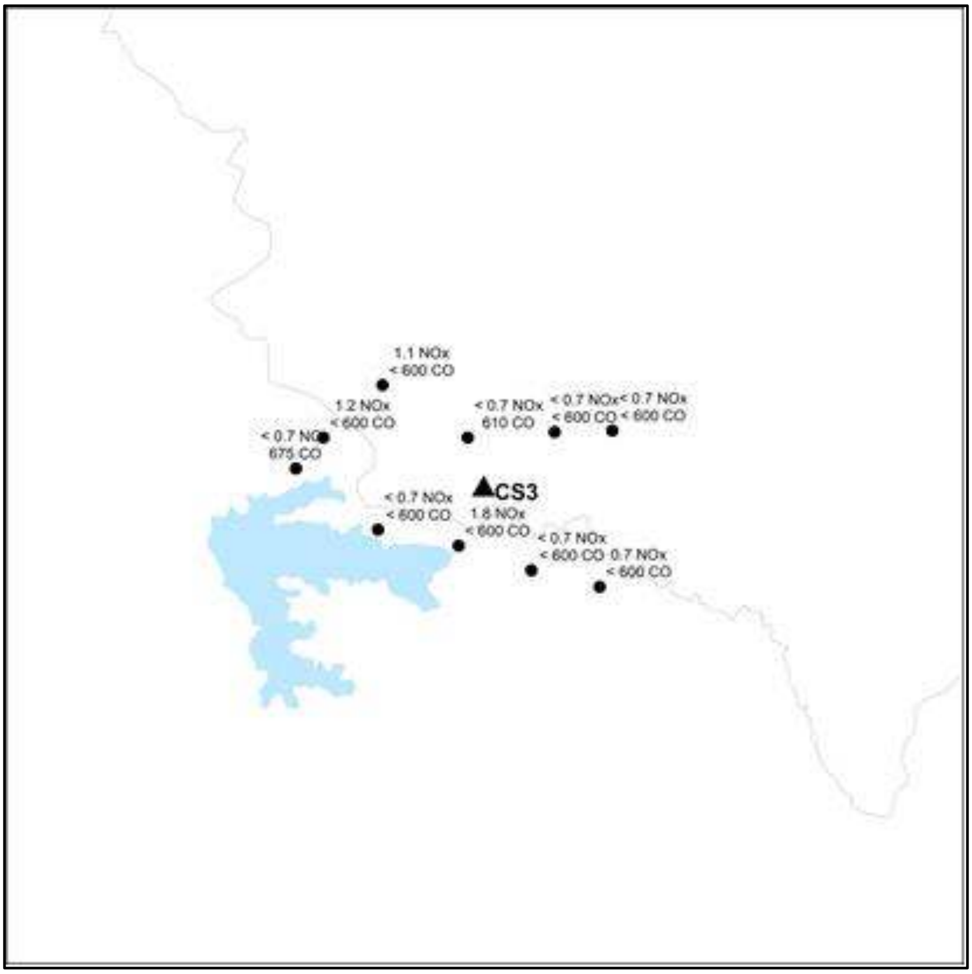


Prepared by Demokritos on behalf of ASPROFOS, 2022.

Figure A2-5 Map of sampling locations in the domain of Achaia (CS3).

Table A2- 6 Field campaign concentration measurements of NOx and CO at locations in the vicinity of CS3.

| Sampling location | NOx (μg/m$^3$) | CO (μg/m$^3$) |
|---|---|---|
| PORTES | <0.7 | <600 |
| PORTES DUPLICATE | <0.7 | <600 |
| GALAROS | <0.7 | <600 |
| VALMI | <0.7 | <600 |
| APIDOULA | 0.7 | <600 |
| KALIVAKIA | 1.8 | <600 |
| XENIES | <0.7 | <600 |

| Sampling location | NOx (μg/m³) | CO (μg/m³) |
| --- | --- | --- |
| AETORACHI | <0.7 | 675 |
| DAFNI | 1.2 | <600 |
| KANDALOS | 1.1 | <600 |
| KATO VELITSES | <0.7 | 610 |
| TRAVEL BLANK | <0.7 | <600 |

Prepared by Demokritos on behalf of ASPROFOS, 2022.

Given the significant low values of NOx and CO in the background area of CS3, the modelling calculations were performed without taking into account the ambient concentrations.

#### 9A.2.3.1 Pollutant concentrations from CS3

Table A2- 7 presents the maximum hourly average concentration of $NO_x$ determined for each characteristic weather type. It can be observed that the **maximum hourly average values of $NO_x$ concentrations from CS3 do not exceed the limit of 200 μg/m³ during any characteristic weather type**. More specifically, the maximum hourly average $NO_x$ concentrations remain low and well below the air quality limit. The maximum hourly average concentration of $NO_x$ of 19.4 μg/m³ was found during CWT6 (summer). This value occurred for 1 hour only during the CWT6.

Table A2- 8 shows the maximum hourly and annual average concentrations of $NO_x$ as well as the maximum 8-hour running mean value of CO calculated in the domain, for direct comparison with the legislative limits. It can be deduced that these maximum pollutant values are very low compared to the air quality limits (2008/50/EC).

Table A2- 9 summarizes the maximum hourly average and annual $NO_x$ concentrations as well as the CO maximum 8-hour running mean values calculated by the dispersion model over all the residential areas of the domain at a radius of ~20 km from the centroid of the industrial field. The concentrations of the pollutants are negligible above the residential areas compared to the corresponding air-quality limits.

Table A2- 7 Maximum calculated near surface values of hourly average NOx concentrations from CS3 in the domain per CWT.

| CS3 | |
|---|---|
| CWT | Maximum hourly (mean) NOX concentration (μg/m3) |
| 1 | 5.9 |
| 2 | 6.9 |
| 3 | 10.1 |
| 4 | 8.4 |
| 5 | 13.1 |
| 6 | 19.4 |
| 7 | 6.1 |
| 8 | 9.2 |
| 9 | 8.7 |
| 10 | 12.8 |
| 11 | 9.4 |

Prepared by Demokritos on behalf of ASPROFOS, 2022.

Table A2- 8 Maximum calculated average concentration values of NOx and CO in the domain from CS3 and air quality limits (2008/50/EC).

| Maximum hourly (mean) $NO_X$ concentration (μg/m$^3$) | Annual average $NO_X$ concentration (μg/m$^3$) | Maximum 8-h mean CO concentration (μg/m$^3$) |
|---|---|---|
| (limit 200 μg/m3) | (limit 40 μg/m3) | (limit 10000 μg/m3) |
| 19.4 | | |

Prepared by Demokritos on behalf of ASPROFOS, 2022.

Table A2- 9 Maximum calculated concentration values of NOx and CO from CS3, over the residential areas in the domain of Achaia, for all CWT.

| CS3 | | | | | |
|---|---|---|---|---|---|
| Nu. | Place of residence | Distance from the centroid (km) | Maximum hourly (mean) $NO_X$ concentration (μg/m$^3$) | Annual average NOx concentration (μg/m$^3$) | Maximum 8-h mean CO concentration (μg/m$^3$) |
| | | | (limit200 μg/m$^3$) | (limit 40 μg/m$^3$) | (limit 10000 μg/m$^3$) |
| 1 | ABRAMI | 15.63 | 0.03 | 0.00 | 0.03 |
| 2 | AGIA BARBARA | 8.20 | 0.07 | 0.00 | 0.06 |
| 3 | AGIA MARINA | 8.49 | 0.01 | 0.00 | 0.29 |
| 4 | AGIA TRIADA | 11.95 | 0.07 | 0.00 | 0.02 |
| 5 | AGIOS ATHANASIOS | 12.37 | 0.00 | 0.00 | 0.07 |
| 6 | AGIOS CHARALAMBOS | 12.34 | 0.13 | 0.00 | 0.33 |
| 7 | AGIOS DIMITRIOS | 11.88 | 0.10 | 0.00 | 0.09 |
| 8 | AGIOS GEORGIOS | 15.58 | 0.06 | 0.00 | 0.00 |
| 9 | AGIOS ILIAS | 8.79 | 0.05 | 0.00 | 0.07 |
| 10 | AGIOS KONSTANTINOS | 11.44 | 0.05 | 0.00 | 0.19 |
| 11 | AGIOS NIKOLAOS | 8.95 | 0.16 | 0.00 | 0.03 |
| 12 | AGNANTA | 13.71 | 0.07 | 0.00 | 0.01 |
| 13 | AGRAPIDOCHORI | 3.33 | 0.61 | 0.02 | 0.36 |
| 14 | ANO VELITSES | 3.01 | 0.23 | 0.01 | 0.17 |
| 15 | ANTHON | 11.72 | 0.05 | 0.00 | 0.02 |
| 16 | ARLA | 15.44 | 0.05 | 0.00 | 0.08 |
| 17 | AVGI | 8.53 | 0.12 | 0.00 | 0.07 |
| 18 | BORSI | 9.04 | 0.16 | 0.00 | 0.25 |
| 19 | CHARAVGI | 7.87 | 0.10 | 0.00 | 0.04 |
| 20 | CHAVARI | 16.27 | 0.01 | 0.00 | 0.03 |
| 21 | CHIONA | 17.04 | 0.05 | 0.00 | 0.03 |

| CS3 | | | | | |
|---|---|---|---|---|---|
| Nu. | Place of residence | Distance from the centroid (km) | Maximum hourly (mean) $NO_X$ concentration (μg/m$^3$) | Annual average NOx concentration (μg/m$^3$) | Maximum 8-h mean CO concentration (μg/m$^3$) |
| | | | (limit200 μg/m$^3$) | (limit 40 μg/m$^3$) | (limit 10000 μg/m$^3$) |
| 22 | DAFNI_A | 12.05 | 0.01 | 0.00 | 0.05 |
| 23 | DAFNI_B | 5.60 | 0.11 | 0.00 | 0.33 |
| 24 | DAFNIOTISA | 11.97 | 0.04 | 0.00 | 0.04 |
| 25 | EFIRA | 8.04 | 0.23 | 0.00 | 0.10 |
| 26 | FLOKAS | 14.32 | 0.13 | 0.00 | 0.09 |
| 27 | GERAKI | 19.45 | 0.02 | 0.00 | 0.04 |
| 28 | ILIDA | 14.35 | 0.03 | 0.00 | 0.10 |
| 29 | INOI | 9.84 | 0.09 | 0.00 | 0.03 |
| 30 | KAGKADI | 14.95 | 0.00 | 0.00 | 0.12 |
| 31 | KAKOTARI | 17.21 | 0.08 | 0.00 | 0.01 |
| 32 | KALFAS | 6.49 | 0.17 | 0.00 | 0.06 |
| 33 | KALIVAKIA | 1.99 | 1.88 | 0.13 | 1.31 |
| 34 | KAMPOS | 7.10 | 0.13 | 0.00 | 0.19 |
| 35 | KANDALOS | 3.43 | 0.58 | 0.01 | 0.75 |
| 36 | KARIA | 15.92 | 0.04 | 0.00 | 0.03 |
| 37 | KARPETA | 11.31 | 0.09 | 0.00 | 0.04 |
| 38 | KEFALAIIKA | 12.01 | 0.06 | 0.00 | 0.07 |
| 39 | KENTRO | 8.66 | 0.20 | 0.00 | 0.15 |
| 40 | KERAMIDIA | 10.94 | 0.05 | 0.00 | 0.06 |
| 41 | KOUTSOCHERA | 14.95 | 0.12 | 0.00 | 0.05 |
| 42 | KRIONERO | 13.76 | 0.06 | 0.00 | 0.04 |
| 43 | LAGANAS | 10.64 | 0.14 | 0.00 | 0.06 |
| 44 | LATAS | 5.47 | 0.28 | 0.01 | 0.13 |
| 45 | LOUKAS | 14.90 | 0.08 | 0.00 | 0.03 |
| 46 | MANESI | 13.37 | 0.14 | 0.00 | 0.04 |
| 47 | MATARAGA | 12.13 | 0.09 | 0.00 | 0.05 |
| 48 | MAZARAKI | 6.82 | 0.21 | 0.01 | 0.08 |

| CS3 | | | | | |
|---|---|---|---|---|---|
| Nu. | Place of residence | Distance from the centroid (km) | Maximum hourly (mean) $NO_X$ concentration (μg/m³) | Annual average NOx concentration (μg/m³) | Maximum 8-h mean CO concentration (μg/m³) |
| | | | (limit200 μg/m³) | (limit 40 μg/m³) | (limit 10000 μg/m³) |
| 49 | MELISSA | 14.84 | 0.00 | 0.00 | 0.40 |
| 50 | MICHIO | 5.69 | 0.19 | 0.01 | 0.08 |
| 51 | MITOPOLI | 19.24 | 0.09 | 0.00 | 0.02 |
| 52 | NEA MANOLADA | 19.54 | 0.01 | 0.00 | 0.04 |
| 53 | NEAPOLI | 14.73 | 0.02 | 0.00 | 0.46 |
| 54 | NEOCHORI | 11.08 | 0.01 | 0.00 | 0.03 |
| 55 | NISI | 12.30 | 0.00 | 0.00 | 0.23 |
| 56 | PANOPOULOS | 17.91 | 0.07 | 0.00 | 0.03 |
| 57 | PERISTERI | 14.62 | 0.04 | 0.00 | 0.01 |
| 58 | PETAS | 14.17 | 0.17 | 0.00 | 0.09 |
| 59 | PIGADI | 12.77 | 0.05 | 0.00 | 0.20 |
| 60 | PIGADIA | 11.95 | 0.02 | 0.00 | 0.03 |
| 61 | PORTES | 3.12 | 0.21 | 0.01 | 0.10 |
| 62 | PRODROMOS | 9.32 | 0.17 | 0.00 | 0.03 |
| 63 | PSARI | 17.21 | 0.01 | 0.00 | 0.15 |
| 64 | RIOLOS | 15.89 | 0.05 | 0.00 | 0.01 |
| 65 | RODIA | 13.38 | 0.07 | 0.00 | 0.04 |
| 66 | ROUPAKIA | 9.78 | 0.06 | 0.00 | 0.02 |
| 67 | SANTOMERI | 7.59 | 0.10 | 0.00 | 0.03 |
| 68 | SIMIZA | 12.65 | 0.02 | 0.00 | 0.15 |
| 69 | SIMOPOULO | 8.85 | 0.11 | 0.00 | 0.03 |
| 70 | SKIADA | 13.66 | 0.07 | 0.00 | 0.03 |
| 71 | SKLIVA | 10.50 | 0.09 | 0.00 | 0.02 |
| 72 | SKOURAS | 10.58 | 0.12 | 0.00 | 0.05 |
| 73 | STAVRODROMI | 12.39 | 0.04 | 0.00 | 0.03 |
| 74 | TSAMEIKA | 9.05 | 0.11 | 0.00 | 0.14 |
| 75 | VELANIDI | 4.97 | 0.22 | 0.01 | 0.20 |

| CS3 | | | | | |
|---|---|---|---|---|---|
| Nu. | Place of residence | Distance from the centroid (km) | Maximum hourly (mean) $NO_x$ concentration (μg/m$^3$) | Annual average NOx concentration (μg/m$^3$) | Maximum 8-h mean CO concentration (μg/m$^3$) |
| | | | (limit200 μg/m$^3$) | (limit 40 μg/m$^3$) | (limit 10000 μg/m$^3$) |
| 76 | VOULIAGMENI | 11.71 | 0.10 | 0.00 | 0.06 |

Prepared by Demokritos on behalf of ASPROFOS, 2022.

Figure A2-6 and Figure A2-7 depict the maximum hourly and annual average concentrations of $NO_x$ from the gas stations, calculated by the model taking into account the 11 characteristic weather types of the region and their frequency of occurrence within a typical year (see Table A2- 2). **It can be deduced, that no exceedances of the $NO_x$ and CO respective air quality limits occur over the populated areas within an approximate distance of 20 km from CS3.** In fact, the maximum hourly (for each CWT) and annual $NO_x$ concentrations are found to be very low compared to the legislative limits (2008/50/EC), (see Table A2- 8, Figure A2-6 and Figure A2-7).

In particular, the maximum hourly average concentration of $NO_x$ of 1.88 *μg/m$^3$* is calculated over the residential area of Kalivakia, which is at the closest distance from the gas stations of ~2 km (air quality limit 200 μg/m3) (see, Table A2- 9). The maximum hourly $NO_x$ concentrations, dispersed to the more distant populated areas of the domain, are not found to exceed the value of 1.0 *μg/m$^3$*, while over most residential sites the concentrations are equal to zero (Figure 5). The maximum annual $NO_x$ concentration of 3.32 *μg/m$^3$* calculated in the area is also very low compared to the respective air quality limit of 40 μg/m$^3$ (see Figure A2-7, Table A2- 8).

A similar conclusion is drawn for the maximum 8-hour running mean CO concentrations, which are found to be negligible compared to the air quality limit (10000 μg/m$^3$, 2008/50/EC). The maximum calculated CO concentration is equal to 11.6 μg/m$^3$ during the CWT6 (summer typical day) (Figure A2-8). The maximum CO concentration calculated over the residential area of Kalivakia is equal to 1.31 μg/m$^3$ (Table A2- 9). Overall, the maximum CO concentrations do not exceed the air quality limit anywhere in the domain and during any characteristic weather type.

**It can be concluded that the modelled $NO_x$ and CO concentrations from the compression station CS3, in the Achaia region, emitted from three identical gas turbines are very low and insignificant compared to the air quality limits of the legislation in force.**

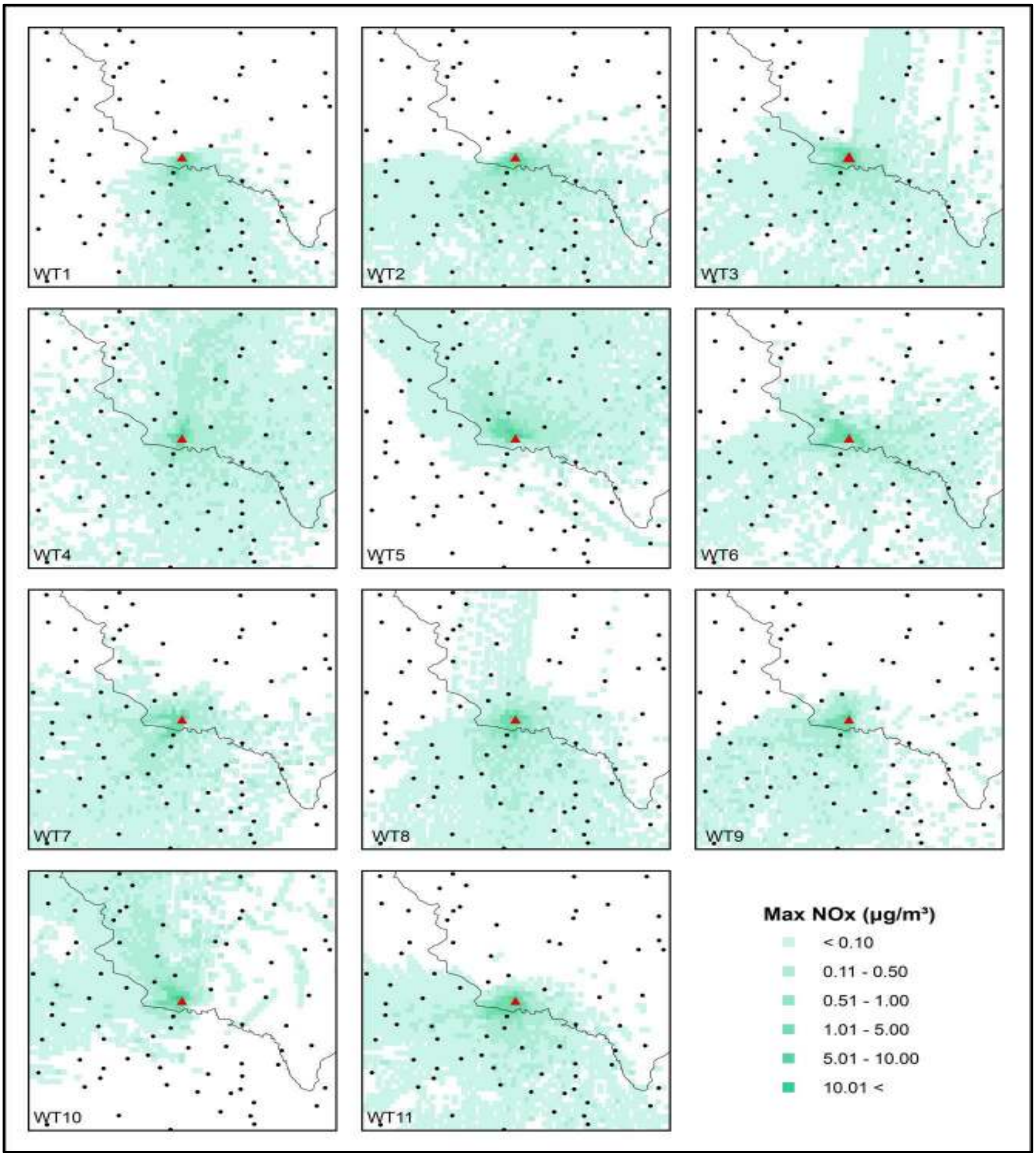


Prepared by Demokritos on behalf of ASPROFOS, 2022.

Figure A2-6 Modelled near surface maximum hourly average concentrations of NOx from CS3 (only) for the 11 CWT. Black dots indicate residential areas, red triangle indicates the centroid of the industrial field. Air quality limit values for hourly concentration of NO2: 200 (μg/m3).

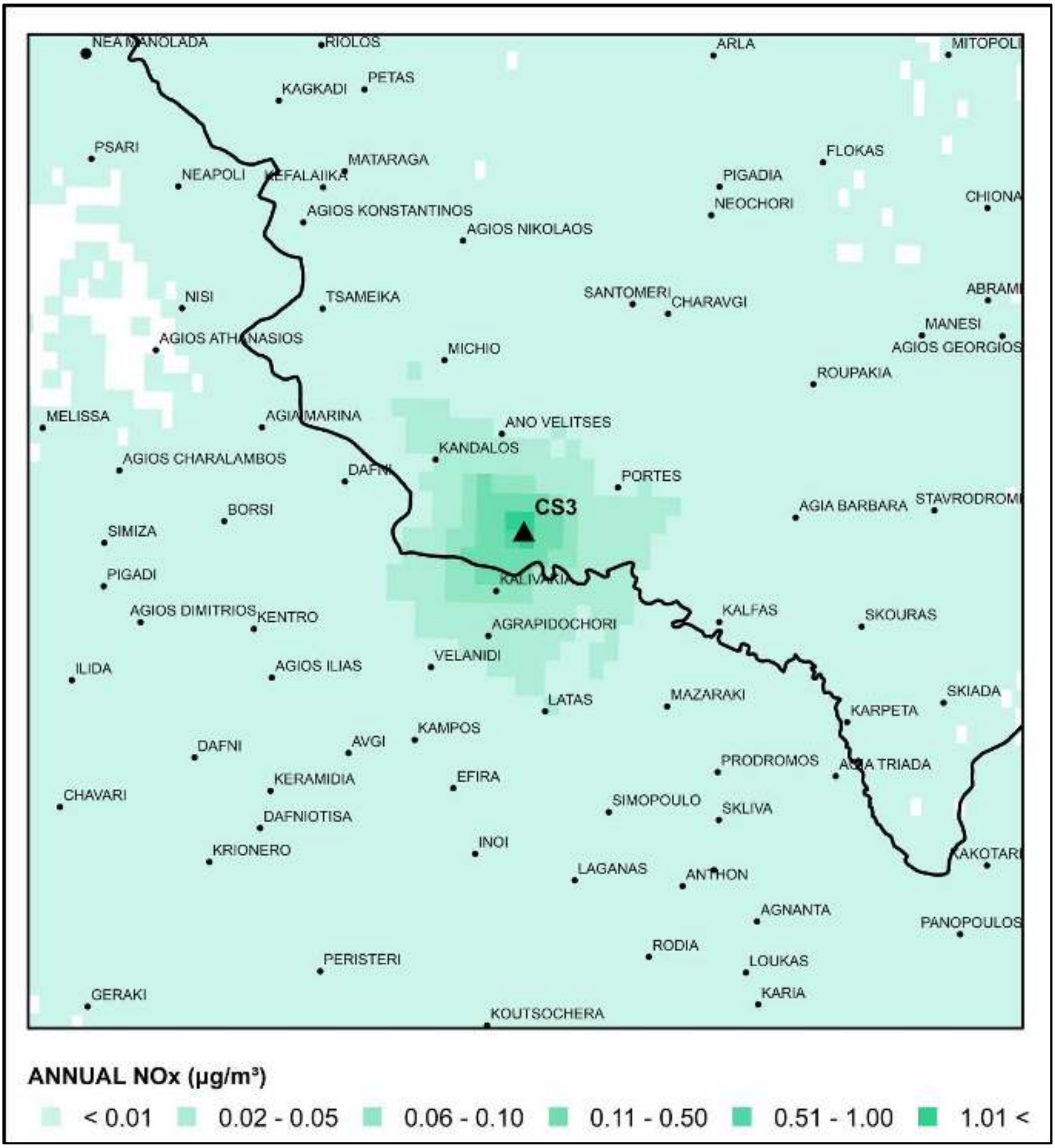


Prepared by Demokritos on behalf of ASPROFOS, 2022.

Figure A2-7 Modelled near surface total average annual NOx concentration contours from CS3 (in μg/m3). Annual Air Quality Limit for NO2: 40 (μg/m3).

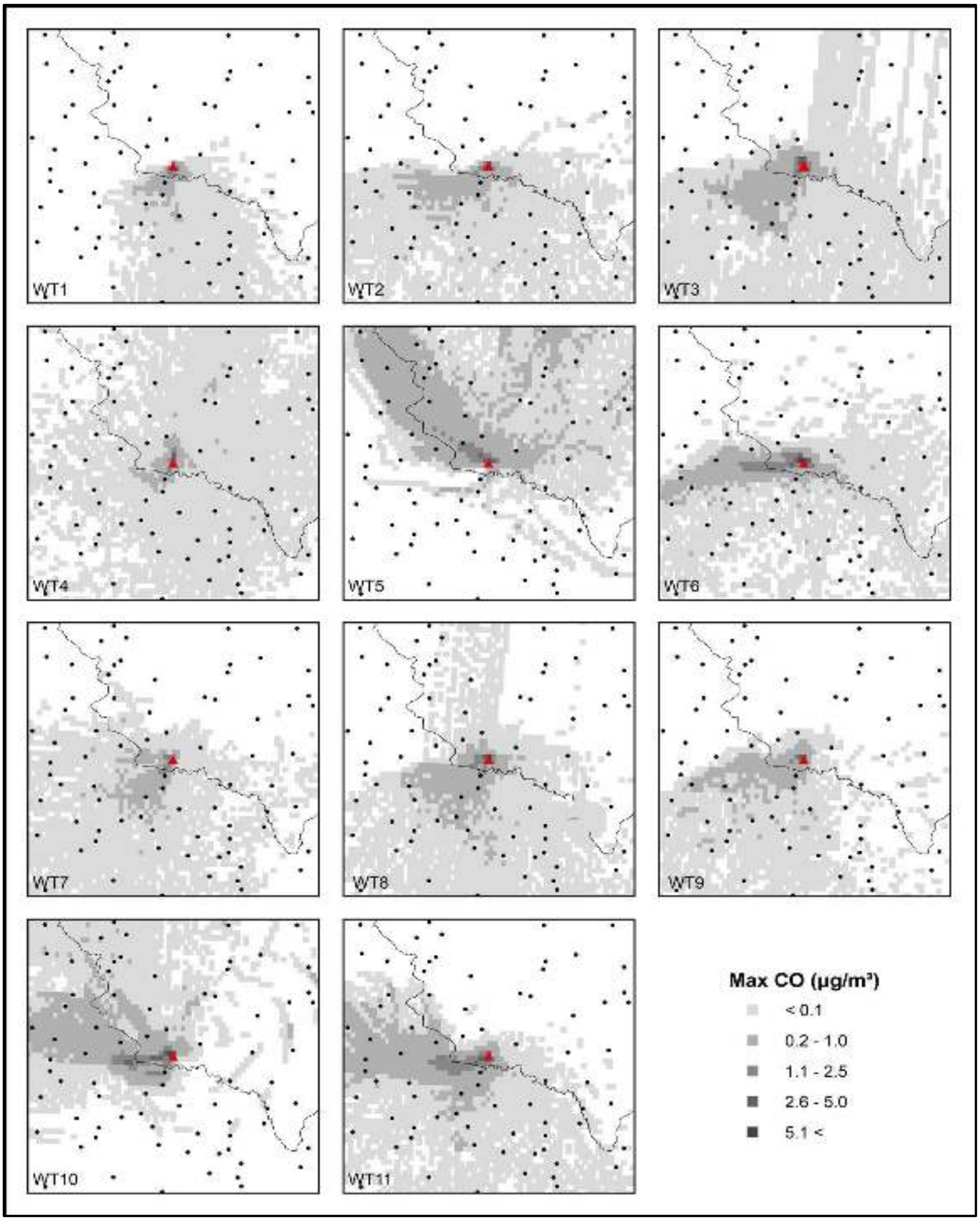


Prepared by Demokritos on behalf of ASPROFOS, 2022.

Figure A2-8 Modelled near surface calculated 8-hour running mean concentration values of CO (μg/m3) CS3 for the 11 CWT. Red triangle indicates the centroid of the industrial field. Air quality limit for 8-hour concentration: 10000 (μg/m3).

## 9A.2.4 SUMMARY – CONCLUSIONS

The aim of the current study was to investigate the dispersion of $NO_x$ and CO emissions from the future gas compressor station CS3 in the area of Achaia (western Greece, north-western Peloponnese). The study was performed with the 3-dimensional computer modelling tools and appropriate methodology used and developed by the Environmental Research Laboratory (EREL) of the NCSR “Demokritos”. The contribution of the measured ambient concentrations of $NO_x$ and CO were not taken into account in the dispersion simulation as the dedicated field campaign revealed significant low values and mostly below the detection limits of the measuring devices. The dimensions of the modelling domain were large enough to include sufficiently the residential areas within a reasonable distance from the gas compression station. Thus, the domain size for the modelling calculations was set to 30 × 30 $km^2$. For the modelling needs, the initial meteorological data were retrieved from the European Centre for Medium-Range Weather Forecasts (ECMWF) ERA-5 climate *high-resolution reanalysis* of 3-hours, covering in total eleven (11) years. To calculate the average levels and the maximum values of the pollutant concentrations in the atmosphere from the future installations on an annual, daily and hourly basis, the procedure of identifying the characteristic weather types (CWT) of the area of interest was followed. The analysis revealed eleven (11) characteristic weather types (CWT) in the domain. Using these data as input to the WRF atmospheric model, the 3-d meteorological fields were calculated with a horizontal and temporal resolution of 1 × 1 $km^2$ and 1-hour, respectively.

For the air dispersion calculations, the atmospheric dispersion model HYSPLIT (Hybrid Single Particle Lagrangian Integrated Trajectory Model) was employed. The modelling was based on the technical information available at the stage of the study by ASPROFOS SA. The background concentrations of $NO_x$ and CO were not considered in the modelling study as the field measurements in the area of the compression station were found to be negligible for a meaningful assessment.

The near-surface hourly average and annual $NO_x$ concentrations as well as the 8-hour running mean CO values were calculated in order to be comparable to the respective air quality limits as set by the legislation in force (MD 14122/549/E.103/2011 “Measures to improve air quality in compliance with the provisions of Directive 2008/50/EC "on the air quality and cleaner air for Europe" the European Parliament and Council of the European Union of 21 May 2008”).

Overall, the hourly mean and annual $NO_x$ concentrations were calculated to be lower than the air quality limits everywhere in the domain and during all CWTs. Similarly, the CO concentrations were calculated to be negligible compared to the air quality legislative limit. The maximum pollutant concentrations were found to occur during CWT6 due to conditions that resulted from the combination of great atmospheric stability and weak wind fields, in late night hours. It must also be emphasised that no exceedances of the NO2 and CO respective air quality limits were found over the populated settlements within a distance of approximately 20 km due to the emissions from the gas compressor station.

Conclusively, the modelling study yielded the following results:

- The maximum mean hourly $NO_x$ concentration was found to be equal to ~9.7% of the air quality limit of 200 μg/$m^3$ (during CWT6, summer period).
- The maximum annual $NO_x$ concentration was found to be equal to 8.3% of the air quality limit of 40 μg/$m^3$.
- The maximum 8-hour running mean CO concentration was found to be equal to 0.12% of the air quality limit of 10000 μg/$m^3$ (during CWT12, winter period).